UNITED NATIONS EDUCATIONAL, SCIENTIFIC AND CULTURAL ORGANIZATION
INTERNATIONAL ATOMIC ENERGY AGENCY
INTERNATIONAL CENTRE FOR THEORETICAL PHYSICS
I.C.T.P., P.O. BOX 586, 34100 TRIESTE, ITALY, CABLE: CENTRATOM TRIESTE

SMR/930 - 16

"Workshop on El Niño, Southern Oscillation and Monsoon"
15 - 26 July 1996

"Monsoon-SO Coupling: Interaction of Annual Cycle & Internannual Variability"

K.M. LAU
NASA/Goddard Space Center
Greenbelt, MD
USA

Please note: These are preliminary notes intended for internal distribution only.

Monsoon-SO coupling : Interaction of Annual Cycle and Interannual Variability

K.-M. LAU
Climate and Radiation Branch
NASA/Goddard Space Flight Center
Greenbelt, MD 20771

WILLIAM BUA
Department of Meteorology
University of Maryland
College Park, MD 20742

(To appear in *Meteorology and Climate of East Asia and the Western Pacific,* World Scientific Press)

ABSTRACT

Land surface and ocean controls over the coupled monsoon-Southern Oscillation (SO) system are examined in a series of coupled General Circulation Model (GCM)-land surface model (LSM) experiments. It is found that interannual variability of the coupled monsoon-SO system is controlled mainly by anomalous ocean forcing. Consistent with previous studies, strong (weak) monsoons are associated with the cold (warm) phase of the ENSO. SST anomalies allow anomalies in the AM to be communicated globally, while seasonally fixed SST limits the influence of anomalous Asian monsoon (AM) to the Northern Hemisphere generally and the AM region specifically. The relationship of the AM to the SO is further examined in 'phase portraits' which trace the trajectory of the total AM-SO system. Strong asymmetries with respect to the annual cycle are found in the mean behavior of the coupled system in all simulations and in the observations, with the SO responding to the annual cycle forcing in late boreal winter/early spring and the AM during late boreal spring to early summer. On the other hand, the boreal fall to winter response of the coupled system to the annual cycle forcing is linear and symmetric. The winter-to-summer behavior of the coupled system suggests a "capacitor" effect with a slow build-up and rapid discharge of energy. AM-SO anomalies from the mean seasonal cycle seem to be initiated in boreal spring in the presence of anomalous ocean forcing, suggesting that the coupled system may be sensitive to perturbations at that time, as was found by Webster and Yang (1992).

While the effect of land-atmosphere appears to be small on the large scale coupled AM-SO system, its influence on the regional scale is quite significant. Over East Asia, land surface interaction seems to excite a see-saw oscillation in precipitation between ocean and land. The polarity of this oscillation appears to be chaotic being dependent on the large scale circulation forced by SST anomalies and the seasonal cycle, and phase-locked to the late spring/early summer portion of the monsoon cycle.

---

1. Introduction

Previous studies have shown that the major convective heat source associated with the Austro-Asian monsoon migrates back and forth along the land bridges of the Indonesia/Northern Australia, Malaysia and Indo-China to the Bay of Bengal and central Asia (cf., Lau and Chan, 1983 and Meehl, 1987). The heat source is strongest when it is located at its extreme meridional position near 10°S over northern Australia in January-February and near 20-35°N over northern India in June-July. This seasonal variation of the monsoon heat sources may be viewed as a direct response to the annual cycle (AC) of insolation at the earth's surface, which is a *meridionally varying external forcing*, with periodicity of exactly one year.

In addition to a strong annual cycle, the monsoon heat source is subject to large interannual variability (IAV). During the warm phase of the El Nino Southern Oscillation (ENSO), the Indonesia heat source is shifted eastward from its normal position to the equatorial central Pacific. In contrast, during the cold phase of ENSO, the Indonesia convection is intensified but confined to the western Pacific and maritime continent. Hence ENSO may be considered as a predominantly *zonal oscillation* having an irregular cycle of 2-7 years. It is important to note that the irregular cycles of ENSO are the outcome of interactions of a full gamut of physical processes within the monsoon-ocean-atmosphere system including possibly other external controls. It is conceivable that the tropical ocean-atmosphere system alone may have an intrinsic oscillation periodicity quite different from the observed. A full spectrum of periodicities can be generated simply by the nonlinear coupling between an external forcing with fixed periodicity and an oscillation with an intrinsic periodicity through a process known as frequency- or phase-locking (Hilborn, 1994). The resulting periodicity depends on the amplitude of the externally applied frequency and the strength of the coupling to the intrinsic frequency.

The phase locking between the ENSO and the AC of the monsoon is well known. A strong Asian monsoon is often found in the summer season following the warm phase and preceding the cold phase of a tropospheric biennial oscillation which happens to be a harmonic frequency of the ENSO cycle (Shen and Lau, 1995). It is plausible that the annual variation of the Asian monsoon may act as a pace-maker that mediates the interaction of the AC and IAV of the Asian monsoon and ENSO. In this paper we present results of a preliminary analysis of monsoon-ENSO interaction based on the above considerations.

2. Model experiments

We have carried out a series of experiments using the NASA Aries GCM coupled to an interactive "mosaic" biosphere model with Surface-Vegetation-Atmosphere-Transfer (SVAT) schemes. The SVAT scheme allows short-term (including diurnal and synoptic scale) interaction between the atmosphere and various vegetation controls for evapotranspiration (Koster and Suarez, 1994). Four integrations with identical initial conditions are conducted with the following specifications:

ALO-simulation: A 10-year simulation with interactive atmosphere and biosphere, using prescribed SST for the period (1980-1989),

AL-simulation: Same as in ALO, except the SST is prescribed to vary with the climatological annual cycle and the simulation is for 20 years,

AO-simulation: Same as in ALO, except that the coupling between land and atmosphere is disabled, by prescribing the β-function (defined to be the ratio of the actual evapotranspiration to the potential evapotranspiration) with the climatological value of AL

A-simulation: Same as in AO, except that climatological SST is used and the simulation is for 20 years.

These experiments are designed to test the role of interactive land surface vs. SST control on the large scale tropical precipitation and circulation. The most important effect of fixing β is to suppress the short-term (diurnal to synoptic scale) interaction between vegetation control and the atmosphere. In this work, this interaction is also examined from the perspective of an interplay between the AC and IAV of the monsoon-ENSO system.

Two indices one for the monsoon and one for the ENSO will be used in the ensuing analysis. Following Webster and Yang (1992), we define the strength of the large scale monsoon

by M_1 which is the vertical zonal wind shear (U_{850} mb minus U_{200} mb) over the region (40 -120°E, 2- 18°N). In this analysis, we focus only on the SO aspect of ENSO to provide the most direct measure of co-variability between the monsoon and the east-west tropical circulation. As a measure of the large scale east-west mass exchange, we use the surface pressure difference between the tropical eastern Pacific (Galapagos) and Darwin to mimic the Southern Oscillation. The modified SOI is somewhat different from the conventional SOI (Tahiti minus Darwin) to maximize the amplitude of the AC and IAV of SO in the model. An anomaly field is defined with respect to the 10-year climatology. Both the anomaly and the total fields will be used in the analyses.

Both M_1 and the SOI possess strong annual cycle as well as interannual variability as can be seen from Fig. 1 which shows the ALO time series of the zonal wind at 200 mb over the monsoon region used in M1 and the Darwin surface pressure, which contributes to a major part of the M1 and the SOI variability respectively. In the Darwin surface pressure, a reduction in the annual cycle amplitude occurs when the IAV is large i.e., 1982-83, 1986-87. In M1, weak monsoons during 1983, 1987 and 1989 can be discerned by the reduced amplitude of the annual cycle. The relationship between the annual cycle and the IAV will be further examined in more detail subsequently.

3. Impact of land surface vs. SST forcing:

a. The Southern Oscillation

Figures 2a-d show the one-point correlation pattern of anomalous Darwin pressure with sea level pressure everywhere for all four experiments. The most conspicuous feature in ALO and AO is an east-west see-saw across the tropical Pacific ocean. This see-saw indicates an exchange in mass between the eastern and the western Pacific. The effect of interactive land and vegetation control does not seem to have a strong impact on this pressure pattern. The fact that this see-saw is absent in AL and A indicates clearly it is due to the effect of anomalous SST forcing. Interestingly, the correlation pattern for AL and for A depicts an almost zonally symmetric variation with nearly zonally uniform pressure variation across the entire tropical oceanic belt. Also found are negative correlation centers over the northern extratropics. These patterns suggest that, absent the anomalous SST forcing, the tropical atmosphere possesses an intrinsic zonally symmetry see-saw linking the tropics and the extratropics. Comparing AL to A, the effect of interactive land surface processes is to disrupt the uniform pressure distribution across the tropical regions. The extratropical anomaly over the Gulf of Alaska /Aleutian region is enhanced in ALO compare to AL, suggesting that extratropical teleconnection signals associated with the SO may be the result of the regional enhancement of an intrinsic zonally symmetric pressure pattern. However, this enhancement is not found in AO, indicating that it may be sensitive to the large scale circulation pattern set up by the anomalous SST forcing.

b. The Asian monsoon

The anomalous 200mb large scale circulation patterns associated with M1 for the different experiments are depicted in Figs. 3a-d, which show covariance of M1 with anomaly wind vectors everywhere. The relationship of M1 to the upper troposphere South Asia anticyclone can be seen in all four experiments. It is evident comparing ALO and AO with AL and A that the impact of the SST anomaly is to drastically expand the influence of the monsoon circulation to the global domain. In ALO and AO, the monsoon upper tropospheric anomalous easterlies are much stronger. They extend across the entire tropical belt, except over the central Pacific, where a double cyclone straddling the equator can be seen. The double cyclone suggests anomalous cooling over the central Pacific at the time of strong Asian monsoon. This is consistent with previous studies which show that a strong (weak) Asian monsoon is associated with the cold(warm) phase of the tropical ocean-atmosphere system and reduced convection over the equatorial central Pacific (e.g. Rasmusson and Carpenter 1982, Yasunari and Seki 1992, Shen and

Lau 1995 and Lau and Yang 1996). The effect of land processes appear to have little impact on the planetary scale monsoon circulation. When the monsoon system is only subject to seasonal variation in SST as in AL and A, the extent of the monsoon circulation is confined to the South Asian region and the northern hemisphere. In fact, there is no indication of any signal related to monsoon variability in the southern hemisphere in AL and A. Clearly basin-wide anomalous SST forcing is required to extend the influence of the Asian monsoon to the global domain.

c. Monsoon-SO phase portrait

In this section, the monsoon-SO relationship is examined via phase-space portraits describing the total climate state of the tropical ocean atmosphere system projected onto the M1-SOI phase plane (See Fig. 4). Because simulation A is very similar to that of AL, results only for ALO, AO and AL will be shown in Figs. 4b, c and d respectively. For comparison, the phase portrait derived from ECMWF data is also shown in Fig. 4a. The cluster of points in the phase-portrait can be viewed as the attractor-basin for the total climate system projected onto M1 and SOI. Comparing ALO and the observed, it is clear that the model climate states evolve in a similar manner to the observed. The ALO simulation appears to have much less IAV compared to the observed as evident in the close clustering and more repeatable annual trajectories of ALO compared to the observed.

The trajectory of the mean annual cycle (thick solid line) is in reasonable agreement with observation. The annual cycle trajectory is in the shape of a right-angled triangle, and varies in a clockwise sense with time. The implications on the annual cycle revealed by the trajectory is quite intriguing. From December through March, there is a large change in SOI, signifying a reversal in east-west pressure differential, while M1 remains almost constant at very low values. The abrupt growth of the monsoon is characterized by the rapid increase in M1 starting from April through June, while in turn the SOI remains relatively constant. During the peak boreal summer, June through August, the climate trajectory stays at the apex of the attractor basin with maximum M1 and maximum negative SOI. The retreat of the monsoon, represented by the September through December trajectory, indicates an almost linear relationship between M1 and SOI. The annual cycle trajectory suggests very asymmetric behavior of the monsoon-SO system with respect to the Asian monsoon. The SO seems to be responsive to the annual cycle forcing from boreal winter through early spring and the Asian monsoon from late spring to early summer respectively. During the boreal fall to winter, the variations of the monsoon and SO are almost linearly correlated.

For IAV, the warm event of 1982-83 and the cold event of 1988-89 are represented by displacements of the climate orbits to different regions of the phase space, accompanied by a distortion of the annual trajectory. The warm event corresponds to smaller values of M1 and extreme negative values of SOI during the boreal spring. On the other hand, the cold event corresponds to larger values of M1 and extreme positive SOI in boreal winter. It is interesting to note that the points of depart from the attractor basin for the warm and cold event trajectories are found in the boreal spring (near the lower left-hand corner of the attractor basin). This implies that the boreal spring may be the time in which the monsoon-SO system is most sensitive to perturbations. This result is also consistent with the so-called spring predictability barrier noted in previous ENSO predictability studies (Webster and Yang, 1992 and Lau and Yang, 1996). The delayed response exhibited by the Asian monsoon and the SO also suggests the dynamical underpinnings of a "capacitor" effect with a slow build-up/rapid discharge process. The rapid monsoon onset from April to May may be related to inherent dynamic instability of the large scale monsoon flow which is pre-conditioned by the seasonally varying lower boundary conditions (Krishnakumar and Lau, 1996).

Comparing AO to ALO, it is clear that the basic features of the monsoon-SO attractor are unchanged by the interactive land processes. However, if the anomalous ocean forcing is removed as in AL, it is seen that the monsoon-SO attractor is dominated by the annual cycle

trajectories which are nearly repeated every year. This means that the IAV of the monsoon-SO system generated by land-atmosphere interaction alone is relatively small.

d. Effect of land surface processes

While the above results show that the IAV of the monsoon-SO system is not strongly influenced by interactive land surface processes, it does not necessarily follow that land surface processes have no influence on the Asian monsoon on a regional scale. In fact, the effect of land surface interaction is quite pronounced in effecting a shift of the monsoon precipitation from the East Asian continent to the adjacent oceans as shown in the precipitation difference map between ALO and AO (Fig. 5a). However, this reduction of rainfall is accompanied by warmer land surfaces over the interior of the continent consistent with energy balance requirements (Fig. 5b). The reduction in rainfall is not matched by evaporation change over the same region, but is related to a shift in the low level moisture convergence pattern (not shown). Koster and Suarez (1994) have suggested a similar shift in rainfall pattern from land to ocean in previous experiments with the same model may arise from the suppression of diurnal and synoptic scale coupling between vegetation control and atmospheric circulation. However, the present results appear to be contradictory to those of Koster and Suarez (1994) who found that the effect of interactive vegetation control led to *increased* precipitation over land and reduction over the adjacent oceans. This apparent paradox may be explain as follows.

Further analyses (not shown) indicate that there is a preferred see-saw oscillation between the oceanic and the continental rainfall in the Asian monsoon region in the model. A positive feedback between the vegetation control and the atmospheric circulation may lead to strengthening of either polarity of the oscillation. Thus depending on the prevailing circulation conditions imposed by the remote forcing of anomalous SST and the seasonal cycle, the land precipitation could be enhanced or reduced. The above-mentioned see-saw oscillation and its chaotic behavior are quite obvious in the Hovmoller diagram of the ALO minus AO precipitation over the East Asian monsoon region shown in Fig. 6. It can be seen that before the summer of 1983 the oceanic precipitation (0-10^{o}N) is reduced and that over the interior of the Asian continent (north of 20^{o}N) rainfall is somewhat enhanced. After the boreal summer of 1983, the polarity of the see-saw changes with large increase in rainfall over ocean and reduced rainfall over land. The occurrence of the see-saw appears to be phase-locked to the May-June months of the years when they are especially pronounced as in 1985, 86 and 87. Examination of the AL minus A rainfall differences (not shown) indicates that the polarity with increased land and reduced ocean rainfall is preferred, but the phase locking is not as pronounced as in the ALO and AO simulations.

4. Summary discussion

We have identified an attractor basin that suggests dynamical behavior of the monsoon-SO system modulated in different ways by remote SST forcing and interactive land surface processes. Results suggest that the monsoon-SO coupling is consistent with the phase-locking between the annual cycle and an intrinsic oscillation with interannual time scales. The annual cycle of the monsoon-SO system is characterized by asymmetric responses at different phases of the seasonal cycle. The IAV is represented by climate trajectories that are displaced systematically away from the mean trajectories depending on the cold or warm phase of ENSO. The ocean influence on the IAV of the monsoon-climate system is very pronounced. On the other hand, land surface processes are important on a regional basis. Interactive vegetation and land processes may lead to a significant displacement of the monsoon precipitation from land to the adjacent oceans or vice versa via the excitation of a coupled land-atmosphere mode. The onset of this major shift in precipitation pattern appears to be chaotic and phase-locked to the prevailing large scale circulation condition during late boreal spring and early summer season.

Acknowledgment

The authors would like to thank Drs. M. Suarez and R. Koster for providing the model outputs for this analysis and for their helpful suggestions and discussions. The second author BB is supported by NSF Grant XXXXX to the Department of Meteorology, University of Maryland. The NASA Mission to Planet Earth Office also provided partial support.

References

Hilborn, R. C., 1994: Chaos and nonlinear dynamics, *Oxford University Press.* 654 pp.

Koster R. and M. J. Suarez, 1994: The components of a 'SVAT' scheme and their effects on a GCM's hydrological cycle, *Advances in Water Resources*, **17**, 61-78.

Krishnakumar V. and K.-M. Lau, 1996: Symmetric instability of monsoon flows. *Tellus* (in press).

Lau, K. -M. and S. Yang, 1996: The Asian monsoon and the predictability of the tropical ocean-atmosphere system. *Quart. J. Royal Met. Soc.*, (in press).

Lau, K. M. and P. H. Chan, 1983: Short-term climate variability and atmospheric teleconnection from satellite derived outgoing longwave radiation. Part II: lagged correlations. *J. Atmos. Sci.*, **40**, 2752-2767.

Meehl, G. A., 1987: The annual cycle and its relationship to interannual variability in the tropical Pacific and Indian Ocean regions. *Mon. Wea. Rev.*, **115**, 27-50.

Rasmusson, E. M, and T. H. Carpenter, 1983: The relationship between eastern equatorial Pacific sea surface temperature and rainfall over India and Sri Lanka. *Mon. Wea. Rev.*, **111**, 517-528.

Shen, S.-H., and K. M. Lau, 1995: Biennial oscillation associated with the East Asian summer monsoon and tropical sea surface temperature. *J. Meteor. Soc. Japan*, **73**, 105-124.

Webster, P. J. and S. Yang, 1992: Monsoon and ENSO: Selectively interactive systems. *Quart. J. Royal Met. Soc.*, 118, 877-926.

Yasunari, T., and Y. Seki, 1992: Role of the Asian monsoon on the interannual variability of the global climate system. *J. Meteor. Soc. Japan*, **70**, 177-189.

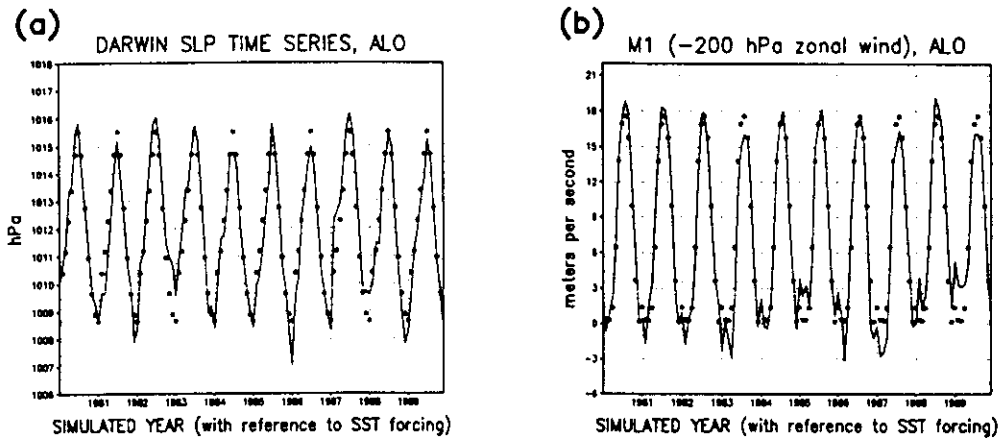

FIGURE 1: Time series showing the annual cycle and interannual variability of (a) zonal wind in meters per second at 200 hPa over the monsoon region (40–110E, 2–18N) and (b) sea level pressure in hPa at Darwin. Solid circles represent the climatological seasonal cycle.

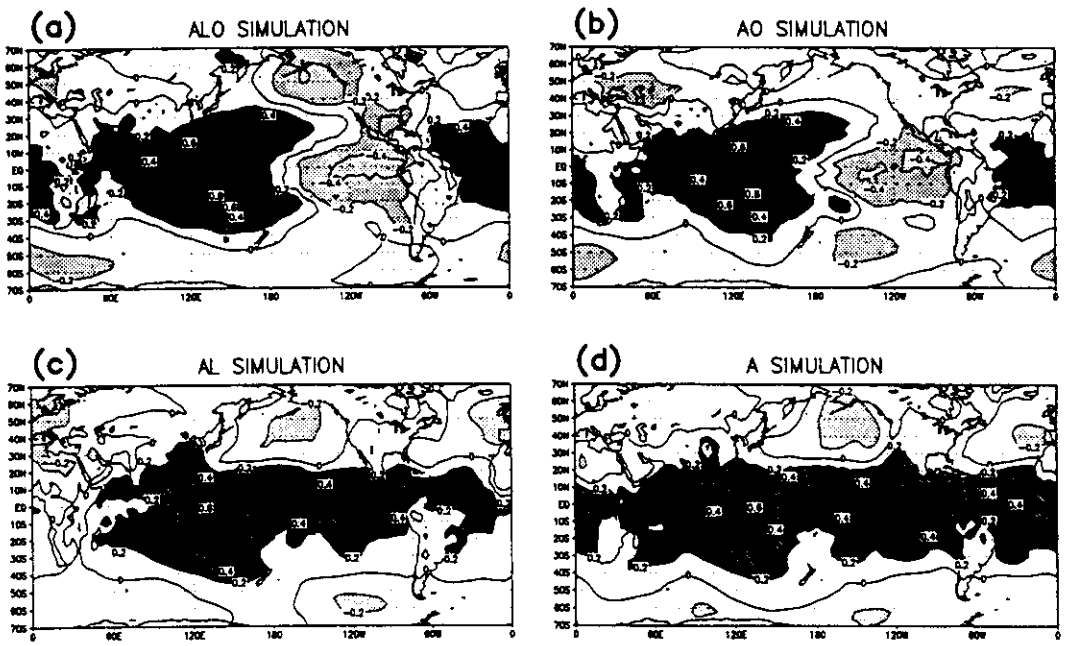

FIGURE 2: One–point correlation between area averaged monthly mean sea level pressure anomalies at Darwin (11S,131E) and gridpoints elsewhere on the globe for the four simulations ALO, AO, AL, and A. Contour interval is 0.2. Areas with absolute value of correlation greater than 0.2 are highlighted.

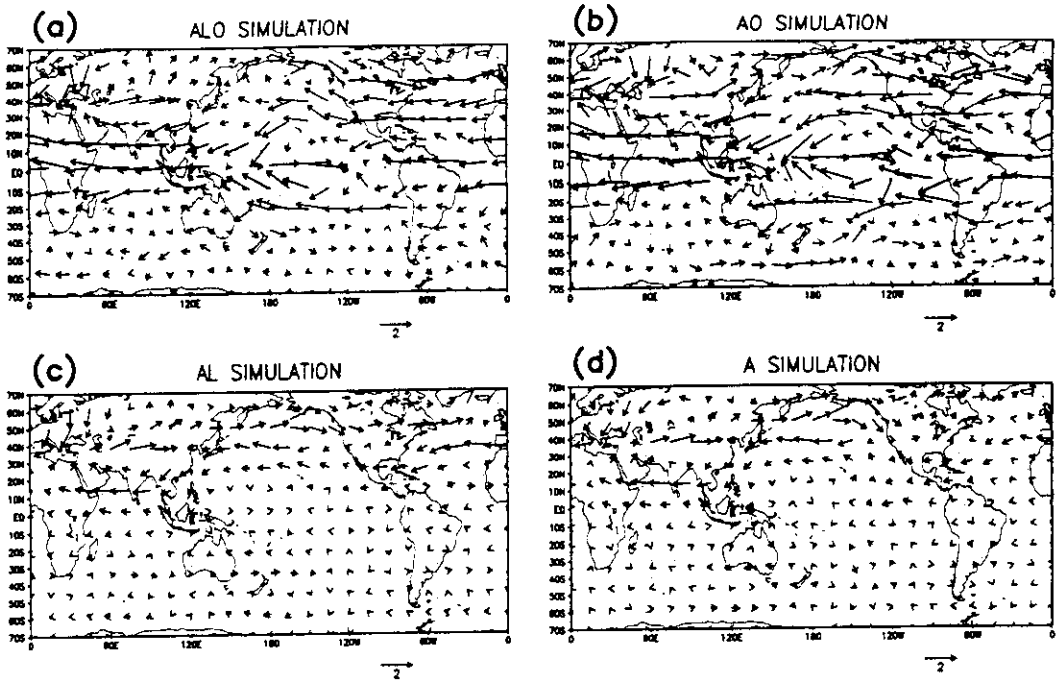

FIGURE 3: Anomaly covariance of monsoon index M1 and 200 mb vector wind at each grid point for ALO, AO, AL, and A simulations. The arrows are scaled as at the lower right of each panel (= 2 meters per second).

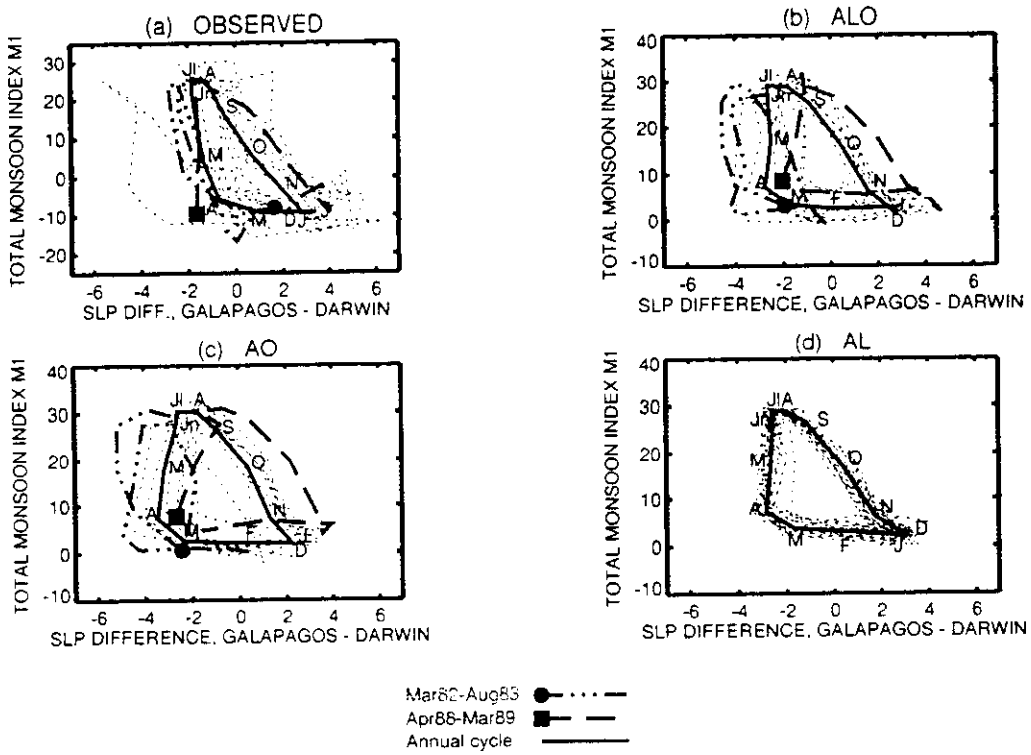

Figure 4: Phase portraits of the monsoon-SO climate system in M1-SOI space for (a) observations from ECMWF data, (b) ALO, (c) AO, and (d) AL. The trajectory for the mean annual cycle is indicated by the black solid line, with each month marked by its first letter.

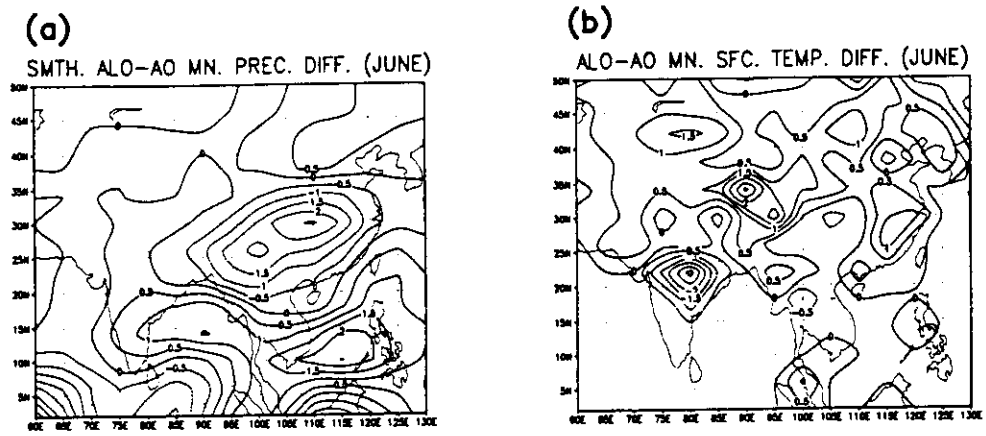

FIGURE 5: Difference maps for ALO minus AO for 10-year June climatology of (a) precipitation in mm per day and (b) surface temperature in Kelvins.

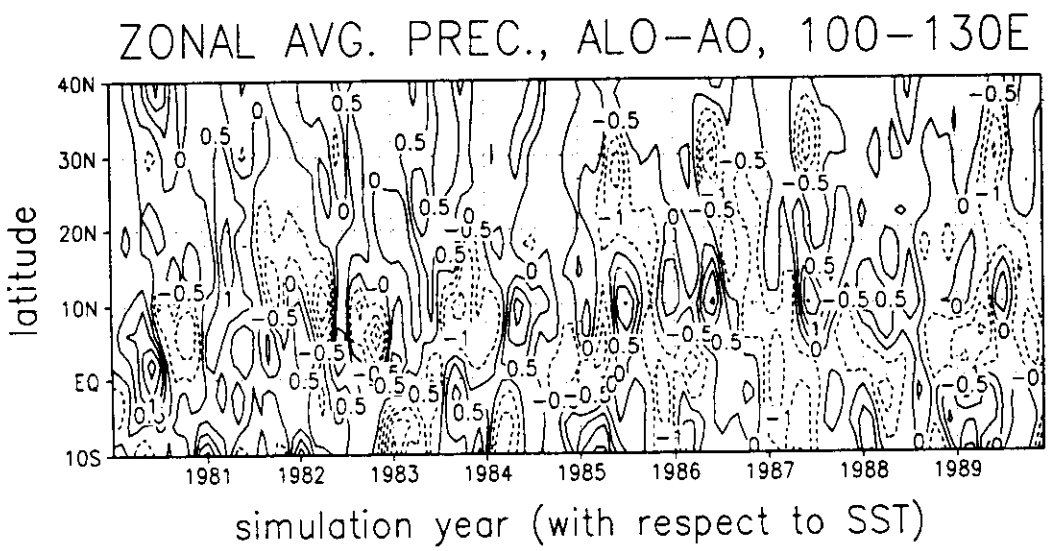

FIGURE 6: Latitude-time Hovmoller diagram for ALO-minus-AO precipitation differences for the entire ten-year integration. Units are in mm per day.